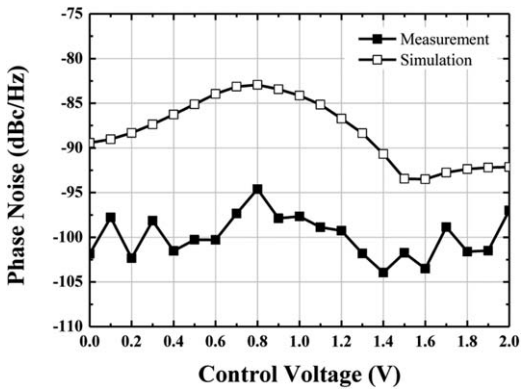


**Figure 8** Measured and simulated phase noise versus tuning voltage

use a single-gate device that is incorporated in the cascode topology.

### 3. EXPERIMENTAL RESULTS

A chip photograph is shown in Figure 4. It has a size of 0.66 × 0.62 mm and includes RF and dc-bias pads. Under a 1.2-V supply voltage, the dc power consumption of the core circuit and buffer are 13.2 mW and 24.8 mW, respectively. Figures 5 and 6 were obtained using the Agilent N9010A EXA signal analyzer. Figure 5 shows an output power of −9.6 dBm, including a cable loss of 4.7 dB. Figure 6 shows the measured and simulated frequencies and output power versus tuning voltage. The measured tuning range is approximately 3.1 GHz and the output power is −4.4 ± 0.8 dBm over the tuning range. Figures 7 and 8 were obtained using the Agilent E5052B signal source analyzer with a Key sight 11970A microwave sub-harmonic mixer. The measured phase noise at 26.5 GHz is −104.0 dBc/Hz at an offset frequency of 1 MHz, as shown in Figure 7. Figure 8 shows that the measured phase noise at an 1MHz offset is around −100 dBc/Hz over the tuning range.

The results of the measurements and of previous work are compared in Table 1. Although there is close correspondence between measured and simulated results for the characteristics of power consumption, output power, and tuning range, the measurement results have low phase performance compared with simulation results. This is because the dual-gate device is modified slightly from the cascode topology in the simulation and its parasitic capacitance and interconnections are not taken into account accurately. According to the experimental results, the proposed VCO shows an FOM and $FOM_T$ [4] of −182 dBc/Hz and −183.1 dBc/Hz, respectively, with a smaller chip area, compared to preciously reported VCOs.

### 4. CONCLUSION

In this paper, a dual-gate cross-coupled VCO was realized using a commercial standard bulk 90-nm 1P9M CMOS process. In order to optimize the phase noise of the VCO, the flicker noise performance of the core dual-gate device was studied in detail. Measurements showed that the dual-gate device had a better flicker noise performance compared to single-gate devices. The proposed VCO achieved a wider frequency tuning range of 3.1 GHz and a low phase noise of less than −95 dBc/Hz at an offset frequency of 1 MHz. These results also showed that the FOM and $FOM_T$ for the phase noise and tuning range were −182 dBc/Hz and −183.1 dBc/Hz, respectively, demonstrating the good performance. The proposed dual-gate-based VCO is suitable for high-performance VCO applications.

**TABLE 1 Performance Summary and Comparison With Differential CMOS VCOs**

| Parameters | [4][a] | [8] | [9] | This Work |
|---|---|---|---|---|
| CMOS process | 65 nm | 130 nm | 130 nm | 90 nm |
| Freq. (GHz) | 25.3 | 23 | 26.3 | 29.2 |
| $P_{RF}$ (dBm) | −1 | −20 | −11 | −3.6 |
| PN@1 MHz (dBc/Hz) | −109 | −109.5 | −92 | −104.0 |
| FTR (%) | 2.81 | 1.5 | 23.6 | 11.2 |
| $P_{diss}$ (mW) | 14.2 | 10 | 43.0 | 13.2 |
| FOM (dBc/Hz) | −185.5 | −186.7 | −174.8 | −182.1 |
| $FOM_T$ (dBc/Hz) | −174.5 | −170.3 | −182.2 | −183.1 |
| Area ($mm^2$) | 0.44 | 0.32 | 1.40 | 0.40 |
| Device | Dual-gate | Single-gate | Single-gate | Dual-gate |

### ACKNOWLEDGMENT

The authors acknowledge the chip fabrication and measurement support provided by the National Chip Implementation Center (CIC) and National Nano Device Laboratories (NDL), Taiwan.

### REFERENCES

1. C.-Y. Hsiao, T.-Y. Su, and S.-H. Hsu, CMOS distributed amplifier using gate-drain transformer feedback technique, IEEE Trans Microwave Theory Technol 61 (2013), 2901–2910.
2. J.-C. Chien and L.-H. Lu, 40 Gb/s high-gain distributed amplifiers with cascaded gain stages in 0.18-mm CMOS, IEEE J Solid-State Circuits 42 (2007), 2715–2725.
3. K. W. Chew et al, Impact of 0.25 μm daul gate oxide thickness cmos process on flicker noise performance of multi fingered deep-submicron mos devices, IEE Proc Circuit Device Syst 148 (2001), 312–317.
4. H. Y. Chang, et al, 65-nm CMOS dual-gate device for *Ka*-Band Broadband low-noise amplifier and high-accuracy quadrature voltage-controlled oscillator, IEEE Trans Microwave Theory Technol 61 (2013), 2402–2413.
5. P. Magnone et al., 1/*f* noise in drain and gate current of MOSFETs with high-k gate stacks, IEEE Trans Device Mater Rel 9 (2009), 180–189.
6. A. Hajimiri and T. H. Lee, Design issues in CMOS differential LC oscillators, IEEE J Solid-State Circuits 34 (1999), 717–724.
7. D. B. Leeson, A simple model of feedback oscillator spectrum, Proc IEEE 54 (1966), 329–330.
8. C. K. Hsieh, K. Y. Kao, J. R. Tseng and K. Y. Lin, A K-band CMOS low power modified Colpitts vco using transformer feedback, In: IEEE MTT-S International Microwave Symposium Digest, Boston, MA, 2009, pp. 1293–1296.
9. K. C. Kwok and J. R. Long, a 23-to-29 GHz transconductor-tuned VCO MMIC in 0.13 μm *cmos*, IEEE J Solid-State Circuits 42 (2007), 2878–2886.



## BANDWIDTH ENHANCEMENT OF RECTANGULAR DIELECTRIC RESONATOR ANTENNA USING CIRCULAR SLOT COUPLED TECHNIQUE

**M. I. A. Sukur, M. K. A. Rahim, and N. A. Murad**
UTM-MIMOS CoE in Telecommunication Technology, Communication Engineering Department, Faculty of Electrical

Engineering, Universiti Teknologi Malaysia, Johor, Malaysia;
Corresponding author: mkamal@fke.utm.my

*Received 9 July 2015*

**ABSTRACT:** *This article presents a technique to enhance the bandwidth of a rectangular dielectric resonator antenna using a circular slot. The structures are designed and simulated using CST Microwave Studio software, and it is found that the circular slot exhibits a bandwidth of 36.44% (0.92–1.33 GHz). The circular slot is compared with the rectangular slot. It is shown that the rectangular slot produces a bandwidth of 6.39% (1.06–1.13 GHz). Both structures exhibit similar radiation patterns with slightly different gains at 3.10 and 3.25 dBi. The bandwidth is enhanced more than five times using the circular slot, compared to the rectangular slot.* © 2016 Wiley Periodicals, Inc. Microwave Opt Technol Lett 58:506–509, 2016; View this article online at wileyonlinelibrary.com. DOI 10.1002/mop.29604

**Key words:** *rectangular dielectric resonator antenna; wideband antenna; circular slot; ultra high frequency*

## 1. INTRODUCTION

The dielectric resonator antennas (DRAs) have been studied numerously due to their advantages: such as high radiation efficiencies, ability to obtain different radiation patterns using different modes [1], the absence of the metal losses, and a relatively compact design with wider bandwidth compared to the microstrip patch antennas [2]. These features, especially when having a relatively smaller size compared to the patch antenna, enable the DRAs to be employed in the UHF band applications. In this band (around 1 GHz), the size of the antennae are large, making it harder to be integrated with the system.

This can be avoided by using a material with high permittivity ($\varepsilon_r$). But by doing this, the bandwidth of the antenna will depreciate. Wide bandwidth is highly desirable, since a single antenna has the capability of replacing multiple narrowband antennas, thus reducing the operational cost. For applications at lower frequency (<1 GHz)—such as walkie-talkie, digital TV and UHF RFID—a compact and low profile antenna is mandatory.

Basically, there are three main shapes of DRA: hemispherical, cylindrical, and rectangular. The rectangular DRA (RDRA) are often used due to the presence of a higher degree of freedom, which enables it to offer more design flexibility [3]. The simplest way to achieve wide bandwidth of the DRA is by using a material with a low $\varepsilon_r$ [4]. Besides that, there are multiple bandwidth enhancement techniques in the DRA design: such as DRA shape modification [5], stacking multiple DRAs [6], hybrid DRA [7], and slotted-fed DRA [8]. The main drawback of these techniques, however, is the excessive size of the DRA. At lower frequency, the slotted-fed DRA is the only technique which can provide wider bandwidth without unnecessarily increasing the size.

The rectangular slot is often used in the slotted-fed antenna configuration. Besides the rectangular slot, there are other shapes of the slot: such as the alphabetical slot, the ring slot, and the circular slot. Previously, the circular slot has been used as a coupler [9], and also as a radiator [10–13]. This was mainly for the ultra wideband (UWB) applications with the ability to obtain a very wide bandwidth—from 3.1 to 10.6 GHz. By utilizing this ability, the circular slot is employed to replace the rectangular slot in the RDRA configuration to enhance its bandwidth. Both configurations employed the same, compact DRA with a dimension of $0.257\lambda_o \times 0.257\lambda_o \times 0.051\lambda_o$ ($L_D \times W_D \times H_D$). Also, the circular slot configuration enhanced the bandwidth by more than five times (more than 30%), compared to the rectangular slot configuration.

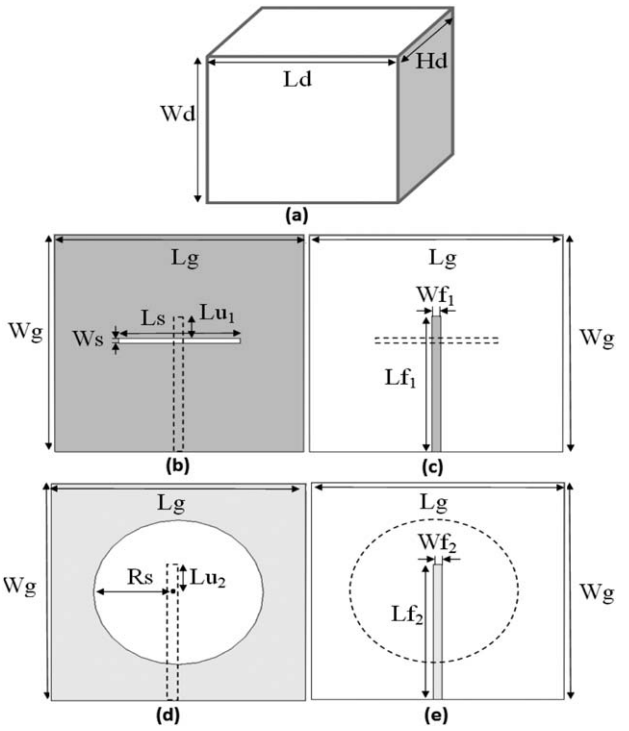


**Figure 1** The proposed antenna configuration: (a) the dielectric resonator. Normal slot configuration: (b) top view, (c) rear view. Circular slot configuration: (d) top view, (e) rear view

## 2. ANTENNA DESIGN CONFIGURATION AND APPROACH

Figures 1(a)–1(e) show the complete proposed antenna design. As shown in Figures 1(b) and 1(d), the dimension of the rectangular slot is 44 mm × 2 mm ($L_s \times W_s$), and for the circular slot, its radius, $R_s$ is 35 mm, which is estimated from the equation in Ref. 13. A dielectric with a permittivity ($\varepsilon_r$) of 7.85 is used for the DRA design. The DRA has a dimension of 70 mm × 70 mm × 14 mm ($L_d \times W_d \times H_d$), as estimated using Ref. 14. The feedline and the ground with the slot are etched on a different side of the Taconic RF35, with a permittivity of 3.5, thickness of 1.52 mm, and a dimension of 90 mm × 90 mm ($L_g \times W_g$). The length and width of the microstrip feedline in both cases are as such to obtain good impedance matching; these are $Lf_1$ = 56.56 mm, $Wf_1$ = 3.17 mm, $Lf_2$ = 56 mm and $Wf_2$ = 3.38 mm. The stub lengths in both cases are indicated by $Lu_1$ and $Lu_2$ which are 9.56 mm and 11 mm, correspondingly. All values are optimal in terms of the impedance matching and bandwidth, and obtained both theoretically and experimentally. The DR is placed in the middle so that the total area occupied can be reduced, and the design analysis can be easily accomplished. In both cases, the broadside fundamental modes of the rectangular DRA, the $TE^x_{\delta 11}$ is excited.

## 3. ANTENNA DESIGN AND ANALYSIS

The parameters of the proposed antenna are determined theoretically from Ref. 14. The design is simulated and analyzed using Computer Simulation Technology (CST) Microwave Studio. Parametric studies are done to obtain the optimal value for all

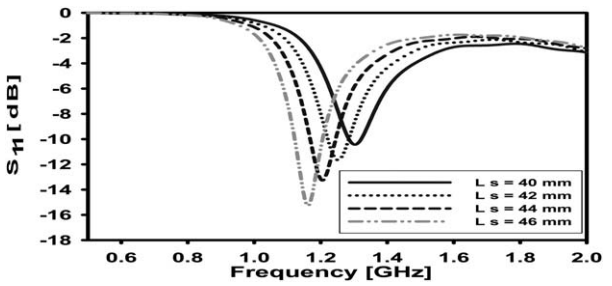


**Figure 2** Comparison of simulated reflection coefficient magnitudes of different slot length (rectangular slot)

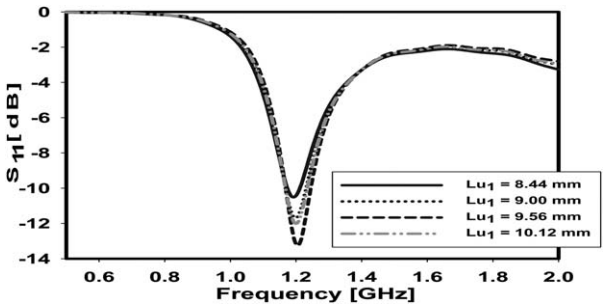


**Figure 3** Comparison of simulated reflection coefficient magnitudes of different stub length (rectangular slot)

the parameters. Some parameters are responsible for the operating frequency, such as the length of the rectangular slot ($L_s$) and the radius of the circular slot ($R_s$), while the others are important so that a good impedance matching can be obtained, such as the length and width of the feedline ($Lf_1$, $Lf_2$, $Wf_1$, and $Wf_2$) and the stub length ($Lu_1$ and $Lu_2$). The dimension of the DRA is determined using the Dielectric Waveguide Model (DWM), assuming that it is radiating in free-space. By setting the operating frequency to 1 GHz ($f_o = 1$ GHz), and maintaining its thickness to 14 mm (as that is the thickness available for the dielectric material), the length and width are 70 mm $\times$ 70 mm.

Figure 2 shows parametric studies for different lengths of rectangular slot ($L_s$). The slot width is kept constant ($W_s = 2$ mm) so that the operating frequency is determined by the slot length. Also, the stub length is kept constant as well ($Lu_1 = 9.56$ mm). As the length of the slot increases, the operating frequency decreases, and the reflection coefficient magnitude ($S_{11}$) improves. The best $S_{11}$ occurred when $L_s = 46$ mm ($-15.29$ dB), and the widest bandwidth occurred when $L_s = 44$ mm (6.61%). Since the bandwidth is

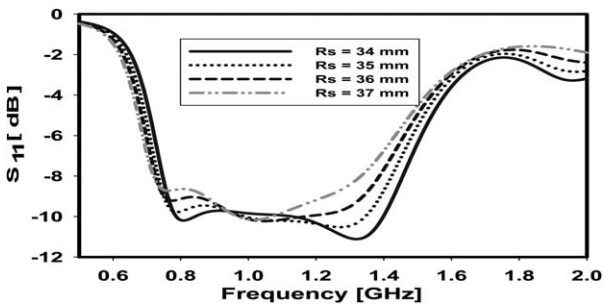


**Figure 4** Comparison of simulated reflection coefficient magnitudes for different slot radius (circular slot)

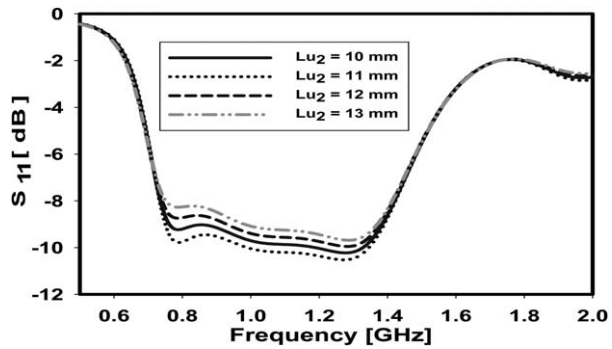


**Figure 5** Comparison of simulated reflection coefficient magnitudes of different stub length (circular slot)

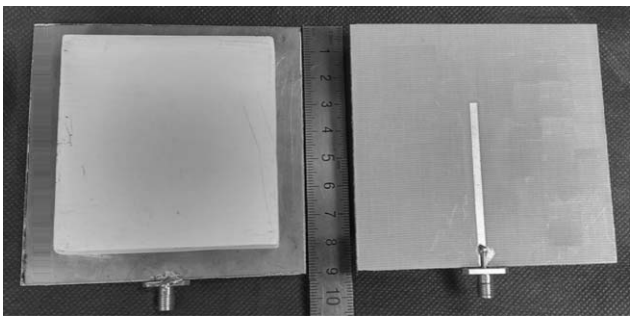

**Figure 6** Fabricated prototypes for both configurations: (a) front view, (b) rear view

the priority in the design, the slot length is chosen to be 44 mm. Figure 3 shows the frequency response as the length of the stub, $Lu_1$, changes. As mentioned before, this parameter is responsible for the impedance matching, so the optimal value of this parameter will give the best $S_{11}$ value and widest bandwidth. The slot length is set to be 44 mm ($L_s = 44$mm), and the optimal value for $Lu_1$ is 9.56 mm.

Figure 4 shows parametric studies on the radius of the circular slot ($R_s$) while setting $Lu_2$ to 11 mm. The widest bandwidth occurred when $R_s = 35$ mm (30.76%). At lower $R_s$, dual-frequency response is achieved—during $R_s = 34$ mm the response merged into one as the radius increases. This may

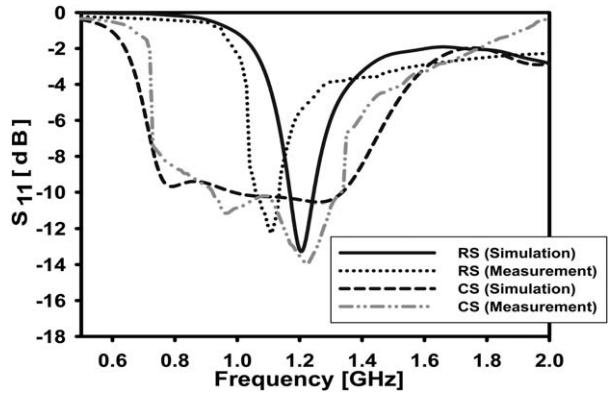


**Figure 7** Comparison of the simulated and measured reflection coefficient magnitude for rectangular slot and circular slot configuration

**TABLE 1 Comparison of the Simulation and Measurement Results for Rectangular Slot and Circular Slot in Terms of the Operating Frequency and the Bandwidth**

| | Parameters | | | | | |
|---|---|---|---|---|---|---|
| | Operating Freq. (GHz) | | | Bandwidth (%) | | |
| Feeding Techniques | Simulation | Measurement | Diff. (%) | Simulation | Measurement | Diff. |
| Rectangular slot | 1.21 | 1.10 | −9.10 | 6.61 | 6.39 | −0.22 |
| Circular slot | 1.17 | 1.13 | −3.42 | 30.76 | 36.44 | + 5.68 |

have been due to the incomplete merging of the response from the slot and the DR, since the radiation pattern produced is different from each other and also from the desired pattern. Similarly, as the first case, the $S_{11}$ value changes as $Lu_2$ changes. As shown in Figure 5, the best $S_{11}$ value occurred when $Lu_2$ is set to be 11 mm. $R_s$ used for this study is 35 mm.

## 4. RESULTS AND DISCUSSION

The antenna with optimal parameters is then fabricated and measured. The prototypes are fabricated using the Taconic RF-35 substrate. Figure 6 shows the fabricated antenna. Only one picture is shown, since both prototypes look the same. The difference lies in the slot configuration underneath the RDRA, as shown in Figures 1(b) and 1(d).

The performance of the prototypes is measured using the network analyzer, and the results are compared with the simulation results to ensure their quality. Figure 7 shows the comparison of the $S_{11}$ between the measured and simulated results for both cases. The acceptable value of the $S_{11}$ is −10 dB, which indicates 90% of the power is transmitted, while the remaining 10% is reflected.

Table 1 shows a summary of the results from Figure 7, specifically in terms of the operating frequency and the bandwidth. In both cases, the operating frequency is shifted to a lower value; about 9.10% for the rectangular slot and 3.42% for the circular slot. Note that the negative sign shows that the frequency is shifted to the left side (lower value). However, the negative sign of the bandwidth result shows that the bandwidth has been degraded, while a positive sign shows that the bandwidth has been increased. The bandwidth of the rectangular slot decreases 0.22%, while the bandwidth of the circular slot increases 5.68%. These differences are expected to come from the fabrication tolerance. They may also be caused by the discrepancies during the process of cutting the DR, cutting the substrate, and positioning the DR in the middle of the substrate. PVA glue is used to stick the DR onto the substrate to obtain a rigid structure. The difference in the bandwidth occurred due the presence of the glue, thus affecting the effective permittivity of the design.

Both configurations have a similar radiation pattern, as shown in Figure 8. The measured and simulation results are in good agreement, despite small differences which might occur due to the positioning of the prototypes and the differences in the radiation power level used during the measurement process. It is clear that both antennas have a bi-directional pattern, by referring to the *H*-plane radiation pattern, with a beamwidth of more than 140 degrees (−3 dB from the maximum magnitude, obtained from the simulation results). The pattern of the antenna

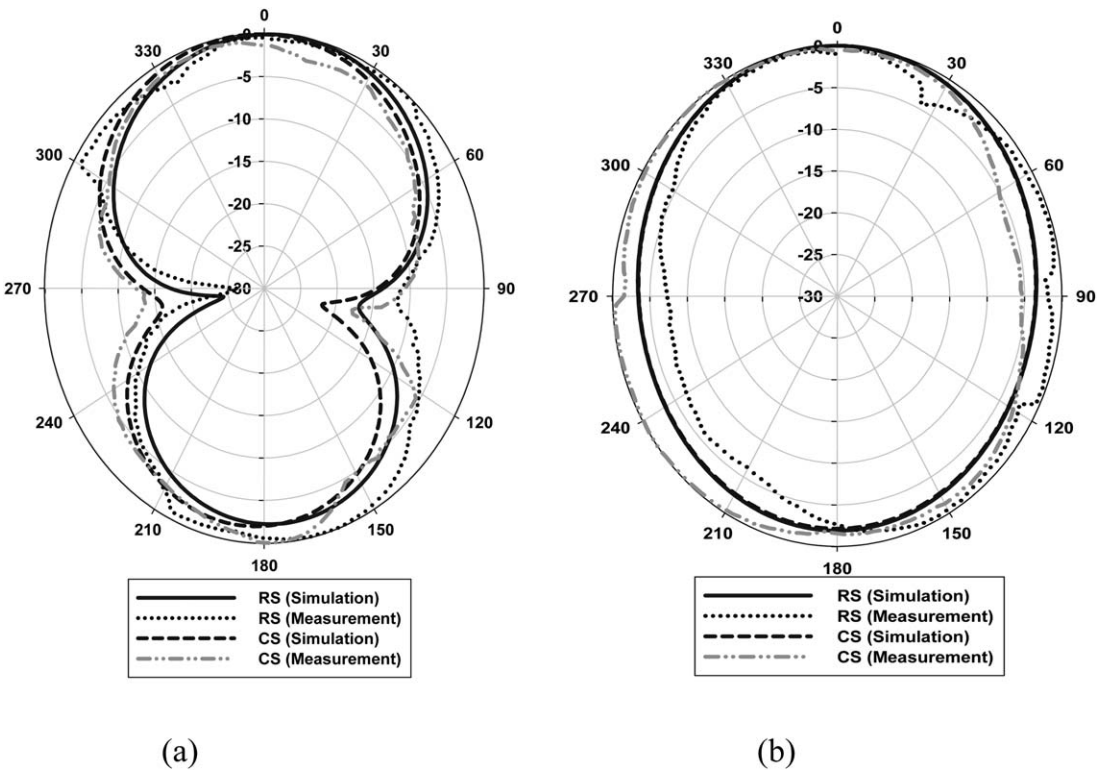


**Figure 8** Comparison of the simulated and measured radiation pattern of the rectangular slot and circular slot: (a) *E*-plane, (b) *H*-plane

**TABLE 2 Comparison Between Simulated and Measured Gain of Rectangular Slot (RS) and Circular Slot (CS) Configurations**

| Gain (dBi) | | Freq. (GHz) | | | | | |
|---|---|---|---|---|---|---|---|
| | | 0.8 | 1.0 | $f_o$ | 1.2 | 1.4 | 1.6 |
| RS | Simulation | −15.42 | −5.14 | 3.81 | 2.81 | −0.40 | −2.88 |
| | Measurement | −2.15 | −0.02 | 3.10 | −3.55 | −8.47 | −10.06 |
| CS | Simulation | −11.30 | 1.48 | 3.96 | 1.02 | −0.40 | −4.62 |
| | Measurement | −12.40 | 0.80 | 3.25 | 1.76 | −10.00 | −6.47 |

is symmetrical, as shown by the *E*-plane, due to the symmetrical configuration of the antenna design. The gain of the antenna is summarized in Table 2.

The gain is inversely proportional to the reflection coefficient magnitude, $S_{11}$, where it is supposedly a maximum at the operating frequency for the narrowband response, and has a positive value throughout the entire bandwidth for wideband response. The maximum gains for both configurations are achieved at their respective frequency, 3.10 dBi at 1.10 GHz for the rectangular slot and 3.25 dBi at 1.13 GHz for the circular slot. Notice that the value of the gain remains positive for the entire bandwidth of the circular slot. The slight differences are due to the differences in the value of the operating frequency between the simulation and the measurement results.

### 5. CONCLUSION

A RDRA has been investigated and fed by two different slots; rectangular and circular. It has been found that by using the RDRA of the same dimension, the circular slot has the bandwidth enhancement capability without significantly affecting other parameters, such as the radiation pattern and the gain. A bandwidth of 36.44% is achieved by the circular slot which is a bandwidth improvement of more than five times compared to only 6.39% achieved by the rectangular slot. Both configurations had gains of 3.10 and 3.25 dBi, respectively.


### ACKNOWLEDGMENTS

The authors thank the Ministry of Higher Education (MOHE) for supporting the research work, Research Management Centre (RMC), School of Postgraduate (SPS), UTM-MIMOS CoE, Communication Engineering Department, and Universiti Teknologi Malaysia (UTMJB) Johor Bahru for the support of the research under grant no 4F360, 05H35, and 4L811.


### REFERENCES


1. R.K. Mongia, A. Ittipiboon, and K.W. Leung, Theoretical and experimental investigations on rectangular dielectric resonator antennas, IEEE Trans Antennas Propag 45 (1997), 1348–1356.
2. B. Li and K.W. Leung, On the differentiality fed rectangular dielectric resonator antenna, IEEE Trans Antennas Propag 56 (2008), 353–359.
3. M. Khalily, M.R. Kamarudin, M. Mokayef, and M.H. Jamaludin, Omnidirectional circularly polarized dielectric resonator antenna for 5.2-GHz WLAN applications, IEEE Antennas Wireless Propag Lett 13 (2014), 443–446.
4. A. Petosa and A. Ittipiboon, Dielectric resonator antennas: A historycal review and the current state of the art, IEEE Antennas Propag Mag 52 (2010), 91–116.
5. K. Mohsen, K.A.R. Mohamad, M. Nor Asniza, S. Noor Asmawati, and A.K. Ahmed, Rectangular ring shape dielectric resonator antenna for dual and wideband antenna, Microwave Opt Technol Lett 55 (2013), 1077–1081.
6. A.A. Kishk, Experimental study of broadband embedded dielectric resonator antenna excited by a narrow slot, IEEE Antennas Wireless Propag Lett 4 (2005), 79–81.
7. A. Mohd Fadzil, O. Ali, and A. Zainal Ariffin, Hybrid dielectric resonator integrated pyramidal horn antenna, Microwave Opt Technol Lett 55 (2013), 1299–1303.
8. A. Buerkle, K. sarabandi, and H. Mosallaie, Compact slot and dielectric resonator antenna with dual resonance broadband characteristics, IEEE Trans Antennas Propag 53 (2005), 1020–1027.
9. M. Leib, A. Vollmer, and W. Menzel, An ultra-wideband dielectric rod antenna fed by a planar circular slot, IEEE Trans Microwave Theory Tech 59 (2011), 1082–1089.
10. A.A. Kalteh, G.R.D. Salleh, M.N. Moghadisi, and B.S. Virdee, Ultra wideband circular slot antenna with reconfigurable notch band function, IET Microwave Antennas Propag 6 (2012), 108–112.
11. A.A. Kalteh, R. Fallahi, and M.G. Roozbahani, A novel microstrip-fed UWB circular slot antenna with 5-GHz band notch characteristics, IEEE Int Conf Ultra Wideband (ICUWB) 1 (2008), 117–120.
12. M. Leib, M. Frei, and W. Menzel, A novel ultra-wideband circular slot antenna excited with a dipole element, IEEE Int Conf Ultra-Wideband (ICUWB) (2009), 386–390.
13. P. Li, J. Liang, and X. Chen, Study of printed elliptical/circular slot antennas for ultrawideband applications, IEEE Trans Antennas Propag 54 (2006), 1670–1675.
14. A. Petosa, Dielectric resonator antenna handbook, Norwood, MA, Artech House, 2007, pp. 29–45.




## A COMPACT FRACTAL UWB ANTENNA WITH RECONFIGURABLE BAND NOTCH FUNCTIONS


**Shrivishal Tripathi,[1] Akhilesh Mohan,[2] and Sandeep Yadav[1]**
[1] Department of Electrical Engineering, IIT Jodhpur, Rajasthan, India; Corresponding author: shrivishal@iitj.ac.in
[2] Department of E&EC, IIT Kharagpur, Kharagpur, West Bengal, India



*Received 10 July 2015*



**ABSTRACT:** *In this paper, a compact reconfigurable single/dual notch band ultrawideband (UWB) antenna with triple notch band characteristics is presented for portable UWB applications. The desired compactness and wideband is achieved using fractals in antenna design. It has the compact dimensions of 24.5 mm × 20 mm. The single/dual notch band reconfigurability is demonstrated in WiMAX band as well as in X-band using two p-i-n diodes for efficient utilization of UWB bands in case of no interference scenarios. The band rejections are obtained by introducing two C-shaped slots in the fractal monopole, whereas band rejection in WLAN band is achieved by placing two C-shaped single split ring resonator on either sides of feed line. In addition, the time-domain characteristic of antenna is also evaluated in terms of fidelity factor, which is more than 0.71. These results illustrates that the presented antenna is appropriate candidate for portable UWB applications.* © 2016 Wiley Periodicals, Inc. Microwave Opt Technol Lett 58:509–514, 2016; View this article online at wileyonlinelibrary.com. DOI 10.1002/mop.29609



**Key words:** *UWB antenna; reconfigurable antenna; fractal geometry; SRR; WLAN; band rejection*


### 1. INTRODUCTION

The ultrawideband (UWB) communication system gets the attention of researchers from academia and industry, after the allocation of 3.1–10.6 GHz frequency spectrum by FCC in 2002 [1]. The UWB band faces the interference issues with the existing narrowband communication systems such as worldwide interoperability for microwave access (WiMAX) in 3.3–3.8 GHz, wireless local area network (WLAN) in 5.15–5.85 GHz and X-band (military communications satellites) in 7.9–8.4 GHz. Thus, the design